Structural analysis of the Interspace Afocal Module of the Wide Angle Viewing System diagnostic for ITER

E. Rincón, S. Cabrera, R. Carrasco, F. Lapayese, M. Medrano, F. Mota, C. Pastor, A. de la Peña, A. Pereira, V. Queral, et al.

Nuclear Materials and Energy 30 (2022) 101127

Contents lists available at ScienceDirect

Nuclear Materials and Energy

journal homepage: www.elsevier.com/locate/nme

Structural analysis of the Interspace Afocal Module of the Wide Angle Viewing System diagnostic for ITER

E. Rincón [a,*], S. Cabrera [a], R. Carrasco [a], F. Lapayese [a], M. Medrano [a], F. Mota [a], C. Pastor [a], A. de la Peña [a], A. Pereira [a], V. Queral [a], F. Ramos [a], C. Rodríguez [a], A. Soleto [a], L. Letellier [b], F. Le Guern [c], J.J. Piqueras [c]

[a] Laboratorio Nacional de Fusión, CIEMAT, 28040 Madrid, Spain
[b] CEA, IRFM, F-13108 Saint-Paul-Lez-Durance, France
[c] F4E, Josep Pla 2, Torres Diagonal Litoral B3, 08019 Barcelona, Spain

ARTICLE INFO

Keywords:
ITER
WAVS
Diagnostic
Structural analysis
FEM
RCC-MR

ABSTRACT

The Interspace Afocal Module (IAM) is one integral component of the ITER Visible/Infrared Wide Angle Viewing System (WAVS), which is an optical diagnostic aimed at monitoring the ITER plasma facing components for machine protection. The diagnostic comprises 15 lines of sight (LoS), strategically distributed in the ITER Equatorial Ports (EP) 3, 9, 12 and 17. Design of WAVS in EP12 is critical, since it has to be fully operational for the first plasma of ITER; it is at its Preliminary stage, carried out by the Consortium constituted by CEA, CIEMAT and Bertin Technologies, within the Framework Partnership Agreement financed by F4E.

The WAVS in EP12 comprises three LoS that pass through the IAM, consisting in a refractive optical system that relays the pupil forward and controls the beam diameter. It includes two doublets of lenses for each LoS, made of Shappire and Calcium Fluoride, with diameters up to 128 mm. The afocal sets (up to 1.9 m in length) are tightly held in place by the support structure of the IAM, which is directly attached to the Interspace Support Structure (ISS).

The IAM structural requirements are highly demanding, given the optical performance that has to be assured under thermal and inertial loads in normal operation, including seismic SL1. In addition, it also has to withstand loads in Category III and IV, including higher seismic events SMHV and SL2, or accidental loads such as the loss of coolant or fire events, since the IAM structure is classified as ITER Safety Relevant, due to its attachment to the ISS.

The paper summarizes the structural analyses performed by CIEMAT to validate the mechanical behaviour of the IAM Preliminary design in EP12, to guarantee both the structural integrity and the optical performance, in accordance with the RCC-MR Code.

Introduction

The Visible/Infrared Wide Angle Viewing System (WAVS) in ITER is an optical diagnostic intended to observe and control the ITER first wall components for the protection of the machine. An overview of the progress in the design and related R&D activities can be found in [1–8].

One essential component of the WAVS is the Interspace Afocal Module (IAM), which consists in a refractive optical system that relays the pupil forward and controls the beam diameter for every line of sight (LoS). The structural requirements of the IAM are highly demanding, given that the optical performance has to be assured under thermal, electromagnetic and inertial loads in normal operation. In addition, it also has to withstand loads in Category III and IV, including higher seismic or accidental loads such as the loss of coolant or fire events.

Therefore, structural analyses are required to guarantee both the structural integrity and the optical performance of the IAM.

Abbreviations: EP, Equatorial Port; IAM, Interspace Afocal Module; ISS, Interspace Support Structure; LC, Load Combinations; LOCA, Loss of Coolant Accident; LoS, Lines of Sight; SL1, Seismic Level 1; SL2, Seismic Level 2; SMHV, Maximum Historically Probable Earthquake; TGCS, Tokamak Global Coordinate System; WAVS, Wide Angle Viewing System.

* Corresponding author.
E-mail address: esther.rincon@ciemat.es (E. Rincón).

https://doi.org/10.1016/j.nme.2022.101127
Received 28 October 2021; Accepted 22 January 2022
Available online 28 January 2022

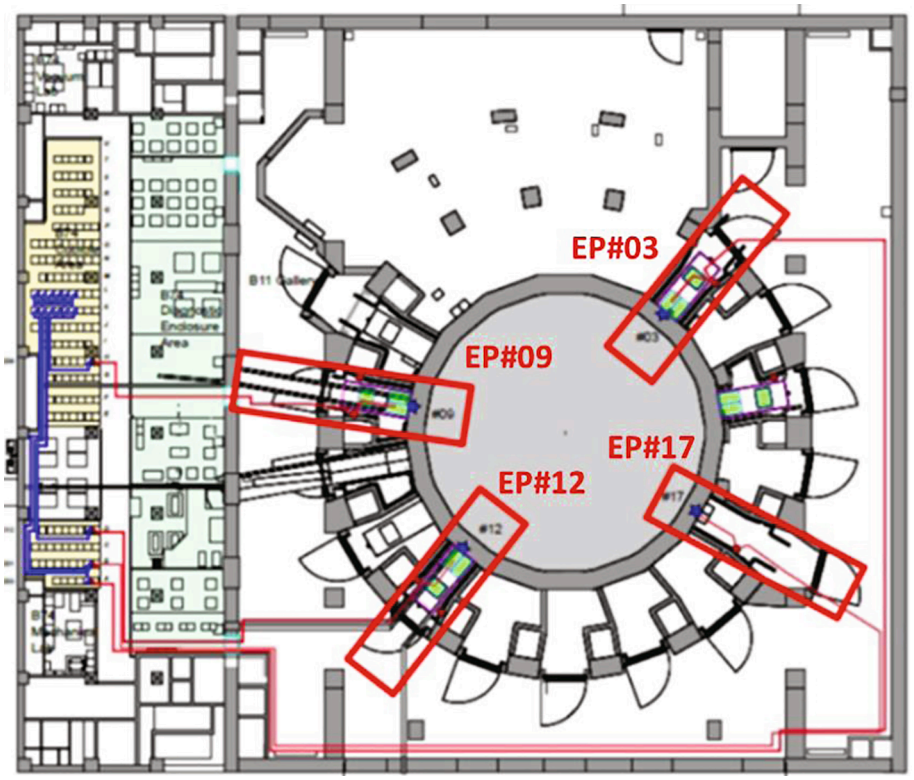

Fig. 1. General layout of ITER WAVS.

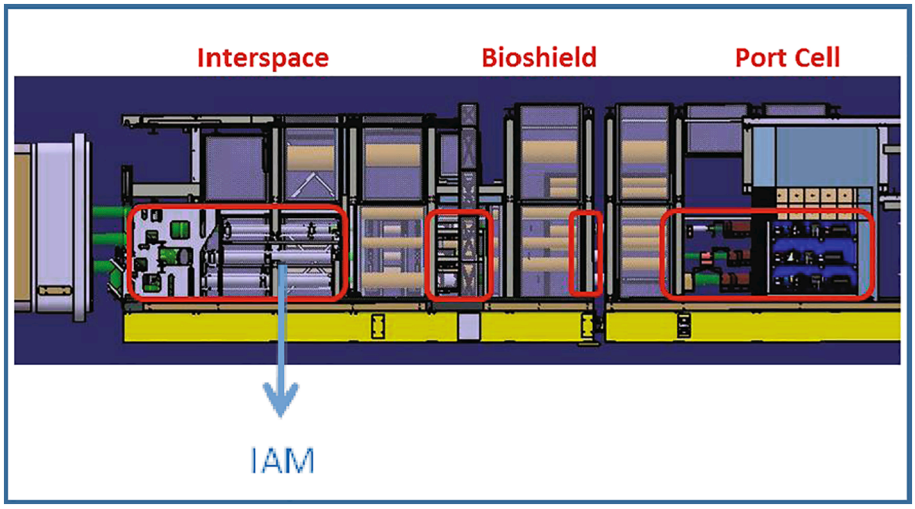

Fig. 2. EP#12 WAVS Ex- vessel components.

This document summarizes the structural analyses performed for the preliminary design of the IAM in the Equatorial Port 12 (EP#12), to guarantee that the component withstand the loads included in the System Load Specifications, also assuring the optical performance in operating conditions. The assessment on the structural integrity of the IAM is made in accordance with the RCC-MR 2007 Code for mechanical components of nuclear installations.

System description

The WAVS comprises 15 infrared and visible lines of sight that are strategically distributed in the ITER Equatorial Ports EP #03, #09, #12 and #17, as shown in the general layout of the Tokamak Building at Equatorial Port level in Fig. 1. This figure highlights the used ports, the cable routes and the position of the WAVS cubicles in the Diagnostic Hall. In EP #03, #09 and #17 there are 4 LoS (two tangential, one upper and one divertor views). However in EP#12, which is the object of this work, there are only 3 LoS (two tangential views and one divertor view).

Fig. 2 shows the location of the WAVS ex-vessel components through the Interspace, Bioshield and Port cell, in EP#12, pointing out the position of the IAM. The ex-vessel components contain the mirrors and refractive elements necessary to relay the exit image of the port plug up to the cameras placed inside a Shielding Cabinet in the Port Cell, covering a length of almost 10 m.

The IAM is represented in Fig. 3, showing the three LoS that correspond to the EP#12. The IAM includes the afocal optics in the

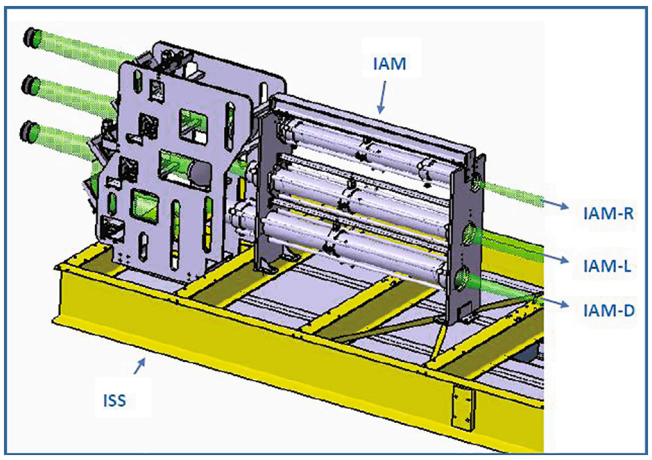

Fig. 3. Interspace Afocal Module (IAM).

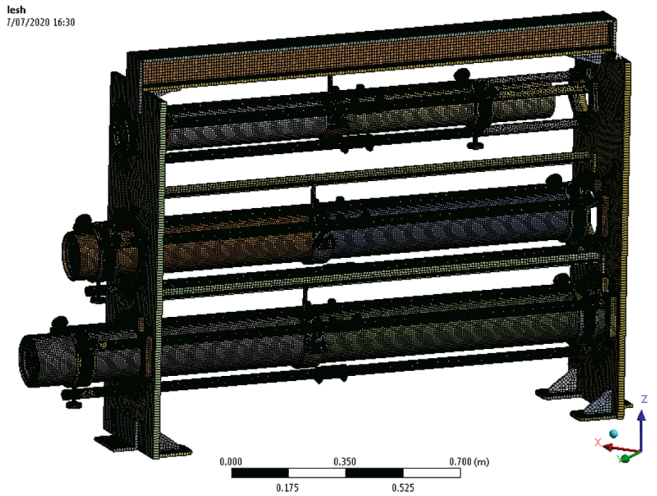

Fig. 4. FE mesh overview of the IAM.

Table 1
Equivalent accelerations.

Acceleration component (TGCS)	SL1	SMHV	SL2
ax (m/s^2)	−4.4	−9.7	−13.3
ay (m/s^2)	−4.1	−9.1	−12.4
az (m/s^2)	14.3	31.2	42.8

Table 2
Applied load combinations.

LC	Mech. Load	Assy. Load	Thermal Load	Seismic Event	Load Cat.
I.1	Gravity	Bolt Preload	18 °C		I
I.2	Gravity	Bolt Preload	35 °C		
II.1	Gravity	Bolt Preload	35 °C	SL-1	II
III.1	Gravity	Bolt Preload	35 °C	SMHV	III
III.2	Gravity	Bolt Preload	LOCA (145 °C)		
IV.1	Gravity	Bolt Preload	35 °C	SL-2	IV
IV.2	Gravity	Bolt Preload	FIRE (300 °C)		

Interspace, which consists of two doublets of lenses for each LoS, mounted at the ends of a Stainless steel SS316L tube, which is up to 1.9 m in length. The lenses are made of Shappire and Calcium Fluoride, with diameters up to 128 mm. The tubes are tightly held in place by the SS316L support structure of the IAM, which in turn is directly attached to the Interspace Support Structure (ISS).

Applied loads

Loads and Load combinations applied in this analysis are compliant with the System Load Specifications approved by ITER for the preliminary design stage. Applied loads include Gravity, Bolt preload, Thermal loads, Seismic events, Loss of coolant accident (LOCA), and Internal fire.

Gravity acceleration is applied to the 356.22 kg mass of the IAM.

Although bolt preloads should not be applied at the preliminary design stage, bolt pretension of 2.7kN has been considered for the M6 bolts in the clamps of the rods and 7.7kN for the M10 bolts in the flanges of the tubes, to ensure that they hold tight the corresponding rods and tubes, so keeping the optical errors of the IAM within the acceptable tolerance range.

Thermal load during normal operation is assumed to be a uniform temperature that ranges from 18 °C to 35 °C.

Since the IAM is classified as Seismic Class 2 (SC-2), Seismic Events corresponding to Level 1 (SL-1), Level 2 (SL-2) and SMHV (Maximum historically probable earthquake) have to be considered. The accelerations applied in the equivalent static analysis are summarized in Table 1 in the Tokamak Global Coordinate System (TGCS).

The only LOCA event that is expected to affect the IAM is the LOCA in the Port Cell, as the atmospheres in the Interspace and Port Cell are shared. Considering that the overpressure has no effect over the IAM, the only load to be applied is a uniform temperature of 145 °C.

Finally, since the IAM support is classified as Safety Relevant, the Internal Fire accidental load has been applied, considering a uniform temperature of 300 °C during 2 h.

Table 2 summarizes the enveloped load combinations (LC) applied in the analyses for every Load Category. LC corresponding to 18 °C has been removed for every load category, since it is enveloped by LC with 35 °C; except for load category I, in which both 18 °C and 35 °C have to be considered to evaluate the optical performance in operating conditions.

Finite element analysis

The analysis has been performed with ANSYS Workbench 2019 *R*3.

The mesh has been verified through the shape testing requested by F4E, showing no errors and only 0.01 % warnings located in non-relevant areas, so assuring the mesh quality. It is mostly composed of 3D hexahedral 20-node solid elements SOLID186, although a proportion of 3D tetrahedral 10-node elements SOLID187 are also required, mainly in transitioning, where the use of hexahedral elements could be problematic or lead to a lesser mesh quality. When possible, non sweepable parts have been divided into several sweepable bodies and mappable surfaces. FE mesh in the IAM support structure is made up of 4-node shell elements SHELL181.

Quadrilateral 8-node surface elements TARGE 174 and CONTA170 have been used for contact simulation.

Element size has been reduced to get the highest quality mesh within acceptable computing time limits, resulting in 1 million elements and 2.8 million nodes (Fig. 4).

Seven independent Static Structural Analyses have been performed, one per each load combination listed in Table 2. The objective of these analyses is to evaluate the stresses and displacements for every load combination, to assess the structural integrity of the IAM preliminary design and to ensure that the optical errors of the IAM in normal

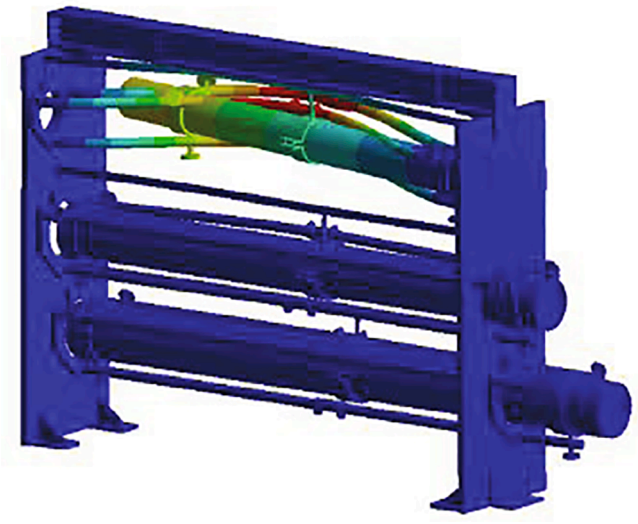

Fig. 5. Mode shape corresponding to the first mode (56.089 Hz).

Table 3
Maximum von-Mises primary stresses.

Load Cat.	Load Combination	Max. VM Primary Stress (MPa)	RCC-MR Elastic Criteria (MPa)
I	Gravity + Preload + 35 °C	39.7	161.3
II	Gravity + Preload + 35 °C + SL1	100.3	161.3
III	Gravity + Preload + 35 °C + SMHV	174.9	217.7
	Gravity + Preload + LOCA(145 °C)	38.6	192.4
IV	Gravity + Preload + 35 °C + SL2	221.2	387.1
	Gravity + Preload + FIRE(300 °C)	37.8	323.1

operation are within the acceptable tolerances.

According to RCC-MR, in order to isolate the primary stresses to assess P-type damage when thermal loads are applied, the thermal expansion coefficient has been set to zero in the material properties, so that the resulting stresses do not include the secondary ones coming from internal loadings, but only the primary stresses coming from external mechanical loads.

In addition to the above Structural Analyses, a Modal Analysis has also been performed to evaluate the natural frequencies of the system, and to confirm that the first natural frequency of the IAM is higher than 33 Hz, according to the limit fixed in the System Load Specifications.

Results I. Structural analysis

In the Modal Analysis, up to 75 modes have been obtained to get a significant participation mass. Fig. 5 shows the mode shape corresponding to the first mode, in which only the upper tube of the IAM is involved, with a frequency of 56 Hz. Therefore, vibration modes of the IAM are acceptable, since the natural frequencies are much higher than the limit of 33 Hz.

In the six independent structural analyses performed for LC I.2 to IV.2 in Table 2, primary stresses have been analyzed to assess the P-type damage, according to the RCC- MR code. Results for maximum von mises primary stresses and the corresponding elastic criteria are summarized in Table 3.

Maximum primary stresses for Category-I are mainly due to the preload of the bolts in the clamps and the bending of the lower rod in the Divertor tube, as represented in Fig. 6.

However, in the other load categories maximum primary stresses are reached for seismic loads, and the maximum values are due to the bending of the rod which withstands the cantilever of the optical tube placed at the bottom of the IAM (Divertor LoS).

Since all the Primary stresses meet the RCC-MR elastic criteria, it can be concluded that the IAM will not be subjected to excessive deformation or plastic collapse for any load combination, so assuring the structural integrity of the component for P-type damage.

Results II. Optical errors

As commented in Section 4, this work is aimed not only to guarantee

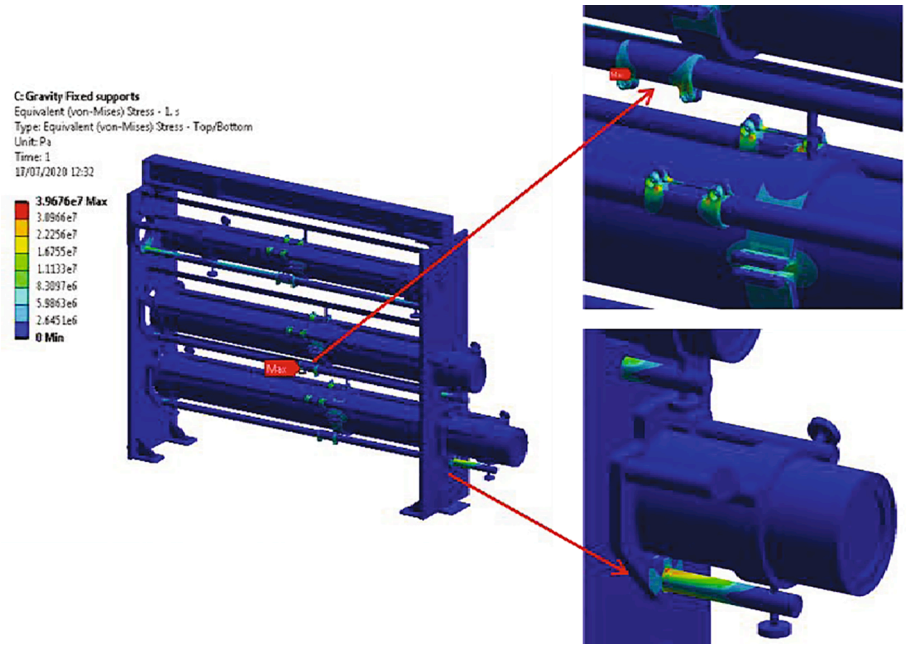

Fig. 6. Primary stresses in LCI.

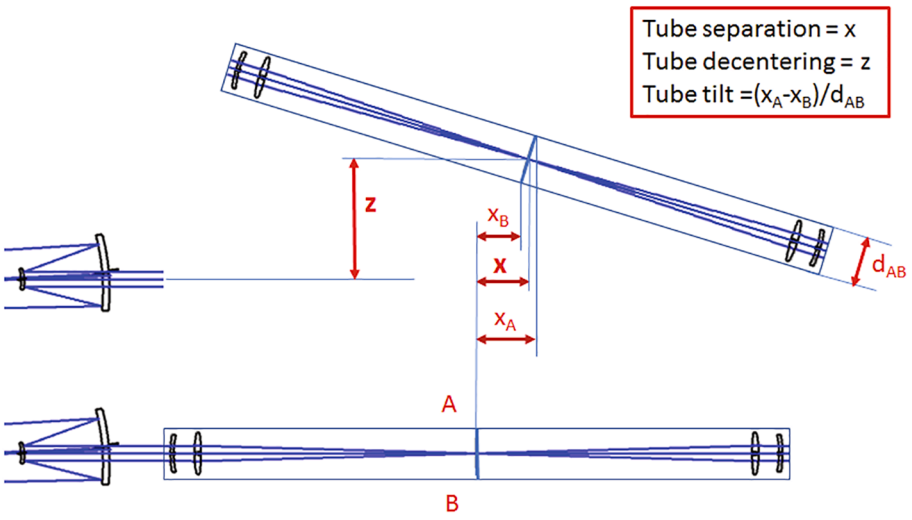

Fig. 7. Residual optical errors in the IAM, considering the tube as a rigid body.

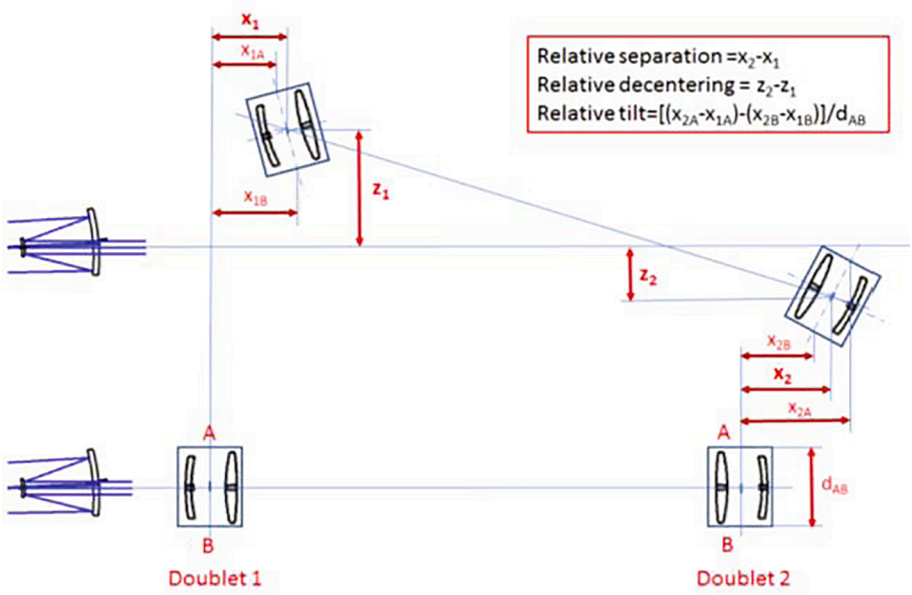

Fig. 8. Relative optical errors between doublets in every tube of the IAM.

Table 4
Criteria and optical errors in the IAM tubes, considered as a rigid body.

		Tilt (arcmin)	Decentering (mm)	Separation (mm)
Criteria		1	0.25	5
IAM-R Tube	18 °C	0.697	−0.164	−0.11
	35 °C	0.688	0.090	0.08
IAM-L Tube	18 °C	−0.061	−0.066	−0.08
	35 °C	−0.052	0.097	0.10
IAM-D Tube	18 °C	−0.295	−0.117	−0.06
	35 °C	−0.286	−0.034	0.11

the structural integrity of the component that has been confirmed in Section 5, but also to ensure the optical performance.

Therefore, thermo-mechanical deformations in operating conditions have been analyzed, since they are the ones that give rise to optical errors. These deformations are mainly driven by thermal loads due to temperature variation from 18 °C to 35 °C in the interspace room.

Optical errors due to these deformations are classified in two groups:

Table 5
Relative optical errors between doublets.

		Relative Tilt (arcmin)	Relative Decentering (mm)	Relative Separation (mm)
Criteria		1.5	0.3	0.5
Doublets in IAM-R Tube	18 °C	−0.079	−0.233	−0.035
	35 °C	−0.075	−0.230	0.262
Doublets in IAM-L Tube	18 °C	−0.192	0.033	−0.049
	35 °C	−0.193	0.029	0.371
Doublets in IAM-D Tube	18 °C	−0.194	0.156	−0.054
	35 °C	−0.194	0.150	0.407

Optical errors in the tube considered as a rigid body (Fig. 7) and Relative optical errors between doublets (Fig. 8).

Optical errors associated to the deformation of the tube, considered as a rigid body, are considered as residual errors that cannot be compensated. They include the tube separation, decentering and tilt, as shown in Fig. 7, in which the deformed tube is represented at the top, and the undeformed one at the bottom.

The criteria for the applicable tolerances to these errors are shown in black in Table 4. This table also includes the results obtained from the thermo-mecanical analyses, showing maximum values in the upper tube (IAM-R) for 18 °C.

On the other hand, the errors shown in Fig. 8 correspond to the relative optical errors between doublets in each tube. They comprise the relative separation, decentering and tilt between doublets, considering the elastic deformation of the tube. Fig. 8 represents the deformed position of the doublets at the top and the undeformed position at the bottom.

The criteria for the applicable tolerances to relative errors are listed in black in Table 5, along with the results obtained from the thermo-mechanical analyses, showing maximum relative errors in the lower tube (IAM-D), for 35 °C.

The values shown in Tables 4 and 5 confirm that optical errors in the IAM meet the criteria, which has been defined taking into account the tolerances applied along the whole ex-vessel optical chain.

Conclusions

The main objective of this work is to assess the preliminary design of the Intespace Afocal Module. As a result of this assessment, the Primary stresses have been found to meet the RCC-MR structural criteria for every load combination. Therefore, the structural integrity of the IAM for P-type damage is assured.

In addition, Bolt metric and preload applied to the bolts in the clamps and flanges have proved to work, both from the mechanical and optical point of view. They hold in place the tubes and rods, so that optical criteria is met, while the stresses created on the clamps and flanges also meet the structural criteria.

On the other hand, Natural frequencies calculated in the Modal analysis are also acceptable, since their values are much higher than the 33 Hz limit defined in the System Load Specifications.

And finally, thermomechanical deformations and the corresponding optical errors calculated for normal operation loads, in which the WAVS system has to maintain service function, also meet the optical criteria.

So in summary, the analyses performed in the Intespace Afocal Module confirm that the preliminary design meets both the optical and the structural requirements.

Disclaimer

The work leading to this publication has been partially funded by Fusion for Energy under Specific Grant Agreement F4E-FPA 407(DG)-SG04. This publication reflects the views only of the author, and Fusion for Energy cannot be held responsible for any use which may be made of the information contained therein.

Declaration of Competing Interest

The authors declare that they have no known competing financial interests or personal relationships that could have appeared to influence the work reported in this paper.

References

[1] S. Salasca, B. Esposito, Y. Corre, M. Davi, C. Dechelle, F. Pasdeloup, R. Reichle, J.-M. Travère, G. Brolatti, D. Marocco, F. Moro, L. Petrizzi, T. Pinna, M. Riva, R. Villari, E.D.L. Cal, C. Hidalgo, A. Manzanares, J.L.D. Pablos, R. Vila, G. Hordosy, D. Nagy, S. Recsei, S. Tulipan, A. Neto, C. Silva, L. Bertalot, C. Walker, C. Ingesson, Y. Kaschuck, Development of equatorial visible/infrared wide angle viewing system and radial neutron camera for ITER, Fusion Eng. Des. 84 (7-11) (2009) 1689–1696, https://doi.org/10.1016/j.fusengdes.2008.12.088.

[2] S. Salasca, H. Arnichand, G. Belhabib, M. Dapena, S. Dastrevigne, C. Dechelle, V. Legrand, Recent technical advancements of the ITER equatorial visible/InfraRed diagnostic, Fusion Eng. Des. 86 (6-8) (2011) 1217–1221, https://doi.org/10.1016/j.fusengdes.2011.02.015.

[3] R. Reichle, B. Beaumont, D. Boilson, R. Bouhamou, M.-F. Direz, A. Encheva, M. Henderson, R. Huxford, F. Kazarian, P.h. Lamalle, S. Lisgo, R. Mitteau, K. M. Patel, C.S. Pitcher, R.A. Pitts, A. Prakash, R. Raffray, B. Schunke, J. Snipes, A. S. Diaz, V.S. Udintsev, C. Walker, M. Walsh, Concept development for the ITER equatorial port visible/InfraRed wide angle viewing system, Rev. Sci. Instrum. 83 (10) (2012) 10E520, https://doi.org/10.1063/1.4734487.

[4] S. Salasca, et al., The ITER equatorial visible/infra-red wide angle viewing system: status of design and R&D, Fusion Eng. Des. 96–97 (2015) 932–937, https://doi.org/10.1016/j.fusengdes.2015.02.062.

[5] L. Letellier, C. Guillon, M. Ferlet, M.-H. Aumeunier, T. Loarer, E. Gauthier, S. Balme, B. Cantone, E. Delchambre, D. Elbèze, S. Larroque, F. Labassé, D. Blanchet, Y. Peneliau, L. Rios, F. Mota, C. Hidalgo, A. Manzanares, V. Martin, F.L. Guern, R. Reichle, M. Kocan, System level design of the ITER equatorial visible/infrared wide angle viewing system, Fusion Eng. Des. 123 (2017) 650–653, https://doi.org/10.1016/j.fusengdes.2017.06.005.

[6] S. Vives, M.H. Aumeunier, C. Guillon, L. Letellier, L. Doceul, M. Proust, C. Portafaix, T. Loarer, N. Lapcevic, N. Lefevre, M. Moll, M. Medrano, V. Martin, F. Le Guern, J. Piqueras, Overview of optical designs of the port-plug components for the ITER Equatorial Wide Angle Viewing System (WAVS), Fusion Eng. Des. 146 (2019) 2442–2445, https://doi.org/10.1016/j.fusengdes.2019.04.014.

[7] C. Pastor, C. Rodríguez, M. Medrano, A. Soleto, R. Carrasco, F. Lapayese, A. de la Peña, E. Rincón, S. Cabrera, A. Pereira, E. de la Cal, F. Mota, F. Ramos, V. Queral, R. Lopez-Heredero, A. Manzanares, L. Letellier, S. Vives, V. Martin, F.L. Guern, J. J. Piqueras, M. Kocan, Optical design of ex-vessel components for the Wide Angle Viewing System diagnostic for ITER, Fusion Eng. Design 168 (2021) 112607, https://doi.org/10.1016/j.fusengdes.2021.112607.

[8] M. Medrano, A. Soleto, C. Pastor, C. Rodríguez, R. Carrasco, F. Lapayese, A. de la Peña, A. Pereira, E. Rincón, S. Cabrera, F. Ramos, E. de la Cal, F. Mota, V. Queral, R. Lopez-Heredero, A. Manzanares, C. Alén-Cordero, L. Letellier, S. Vives, V. Martin, F.L. Guern, J.J. Piqueras, M. Kocan, Design overview of ex-vessel components for the Wide Angle Viewing System diagnostic for ITER Equatorial Port 12, Fusion Eng. Design 168 (2021) 112651, https://doi.org/10.1016/j.fusengdes.2021.112651.